

EFFECT OF GRAIN SIZE ON THE ELECTRICAL TRANSPORT MECHANISM FOR ZINC DOPED CDS THIN FILMS

Awodugba A.O, Ibiyemi A.A and Ajayi J.O

Department of Pure and Applied Physics, LAUTECH, P.M.B 4000, Ogbomosho, Nigeria.

ABSTRACT

Cd_{1-x}Zn_xS (x = 0.0, 0.2, 0.4, 0.6, 0.8 and 1.0) has been prepared by microwave-assisted chemical method using cadmium sulphate, zinc sulphate, and thiourea as the source of Cd²⁺, Zn²⁺ and S²⁻. Films were polycrystalline in nature and oriented preferentially in the 002 direction. Electrical properties have been investigated by Vander pauw four point probe configuration so as to understand the impact of Zn in the electrical transport mechanism. The decrease in conductivity with increase of Zn concentration is attributed to the increase of grain boundary surface area, which is responsible for the decrease of carrier mobility. It is noticed that the lattice structure becomes more and more disordered with the increase of Zn content due to increase in grain boundary scattering. It was observed that conductivity decreased with increasing Zn-content in CdS and results have been analyzed according to the grain-boundary scattering mechanism. Decrease in the electrical conductivity on the incorporation of Zn can be attributed to the maximum amount of grain boundary scattering, which leads to increase of the height of barriers. The decrease of conductivity with a further increase of zinc occurred because Zn²⁺ introduced additional charged scattering centers at the grain boundaries which restrict carriers transport. Charge carrier mobility and carrier concentrations of the films are dependent on the grain size, the film with a smaller grain size has a higher carrier concentration and lower mobility. The electrical conductivity is related to the grain size and shows a maximum for the film with grain size of about 36.445 nm. Activation energy studies were also made. The electrical conductivity measurement was carried out in 300-500 K temperature range. The activation energy is found to be grain size dependent and it varies in the range of 0.096-0.194 eV at low temperature range, 0.247 – 0.7206 eV in middle temperature range and 0.688 to 0.789 eV at higher temperature. Semiconductor behavior was observed from the electrical conductivity measurements. The conductivity measurements reveal that films exhibit n-type conductivity.

I. INTRODUCTION

Cadmium sulphide (CdS) is an important material which can be used to make n-type materials for thin film hetero junction solar cells. Attempts have been made to replace CdS with material which exhibit higher energy band gap such as CdZnS. This attempt has led to decrease in window absorption losses and increase in short circuit current. The grain size tunability of the CdZnS thin films for various Zn²⁺ concentrations was successfully demonstrated in our work. CdZnS has attracted technological interest because the energy gap can be tuned and the lattice parameters can be varied (Ulrich et al, 2000). In CuGaSe₂ heterojunction solar cells, the use of Zn_xCd_{1-x}S led to an increase of photocurrent by minimising the electron affinity mismatch between the two semiconductors. Further, Zn_xCd_{1-x}S can also be used as a window material in the fabrication of p-n junction solar cells without lattice mismatch in the devices based on quaternary materials like CuIn_xGa_{1-x}Se₂ (Yamagushi et al, 1992). It is well known that the electrical and optical properties of semiconducting materials depend strongly on defect density created by external doping as well as their preparation and growth conditions. The addition of trace amount of metal ion such as Zn into CdS plays an important role in modifying the structural, optical and electrical transport properties of the binary alloy material also doping of group III elements has been found to increase the conductivity of CdS thin films (Jae-Hyeong et al, 2003), the efficiency of CdS semiconductor film was improved by changing its optical and/or electrical

properties by doping with some foreign elements such as Gallium, Copper and Aluminum (Jafari et al, 2011). Zn doped CdS thin film has emerged as an important material due to its applications in photovoltaic cell as window layers and as transparent conducting semiconductor for optoelectronic devices, conductivity of CdS thin films decrease after doping with Zn, Zn^{2+} ions tend to replace Cd^{2+} ions in the lattice. However Zn^{2+} ions tend to enter the lattice substitutionally at low concentration, and interstitially at high concentration. Interstitial ions will act as recombination centers increasing the resistivity (Patil et al, 2011). Doped CdZnS films can be deposited by several methods such as Thermal Evaporation, Chemical bath Deposition and Spray Pyrolysis [Abbas et al, (2013) and Kumar et al, (2004)], among all technique spray pyrolysis has been used extensively being large area deposition and chemically viable technique, we have shown that spray pyrolysis is a suitable technique for Zinc doping of CdS. Concentration of the starting material (solution) highly affects the nature of the film mainly its grain size, growth of the film (Asanat et al, 2004).

II. MATERIALS AND METHOD

The $Cd_{1-x}Zn_xS$ thin films were prepared by Microwave-assisted Chemical Bath Deposition technique on commercial glass slide for various zinc concentration ($x= 0.0, 0.2, 0.4, 0.6, 0.8$ and 1.0). The starting materials used were $CdSO_4$ as a Cd^{2+} ion source, $ZnSO_4$ as Zn^{2+} ion source, thiourea as an S^{2-} ion source and NH_4OH complexing to control the Cd^{2+} and Zn^{2+} ion concentrations. An alkaline solution of ammonia was used to adjust pH of the reaction mixture. All the chemicals used were of Analytical Reagent grade. The deposition parameters are present in the table.1. The microscopic glass slides are cleaned using chromic acid for 24 hours at room temperature and placed vertically inside the chemical bath. The deposition was carried out for very short duration 10 minutes when compared to the usual CBD deposition. The Micro wave Oven was set to temperature of $90^\circ C$. After the deposition, the CdZnS films were washed with distilled water ultrasonically to remove the loosely adhered particles on the film and finally dried in air. Thickness was determined using gravimetric method. X-ray diffraction has been used to study the structure and lattice imperfection of the films. Van der Pauw four-point probe configuration was used to evaluate the carrier concentration and carrier mobility.

Table1. Deposition parameters of CdZnS

Compounds	Parameter x	ZnSO ₄ (mol)	CdSO ₄ (mol)	NH ₂ CSNH ₂ (mol)	NH ₄ OH	Temperature (°C)	Time (sec)
Cd _{1.0} Zn _{0.0} S	0.0	0.000	0.250	0.200	0.580	90	600
Cd _{0.8} Zn _{0.2} S	0.2	0.3750	0.250	0.200	0.580	90	600
Cd _{0.6} Zn _{0.4} S	0.4	0.1667	0.250	0.200	0.580	90	600
Cd _{0.4} Zn _{0.6} S	0.6	0.0625	0.250	0.200	0.580	90	600
Cd _{0.2} Zn _{0.8} S	0.8	0.0365	0.250	0.200	0.580	90	600
Cd _{0.0} Zn _{1.0} S	1.0	0.0125	0.000	0.200	0.580	90	600

The crystallographic studies made using X-ray diffraction analysis clearly indicated the effect of alloying on the crystalline quality of the grown layers. The X-ray diffraction spectra of $Cd_{1-x}Zn_xS$ films with different Zn composition are shown in Figure 1-5. The X-ray diffraction patterns of the layers showed the same preferential orientation in the investigated composition range. The X-ray diffraction patterns mainly exhibited peaks related the (100), (002), (101), (102) (110), (103), and (200) orientations of hexagonal structure. All the layers exhibited the (002) crystal plane as the preferential orientation and its intensity increases with the increase of zinc content in the layers. As the samples are originated from hexagonal structure, no phase transition occurred with the increase of Zn/Cd ratio in the films. Some diffraction peaks disappeared with the increase of Zn content.

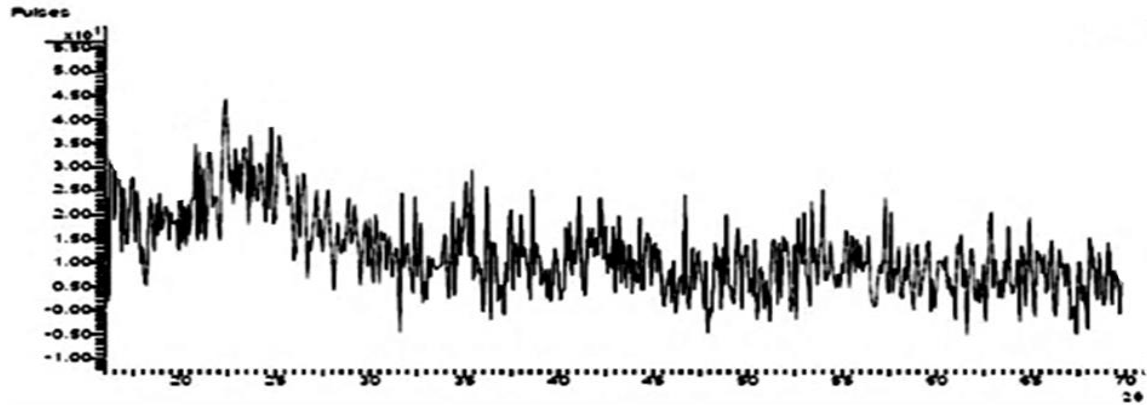


Figure 1: X-ray diffraction pattern of Cd_{0.8}Zn_{0.2}S nano-crystals.

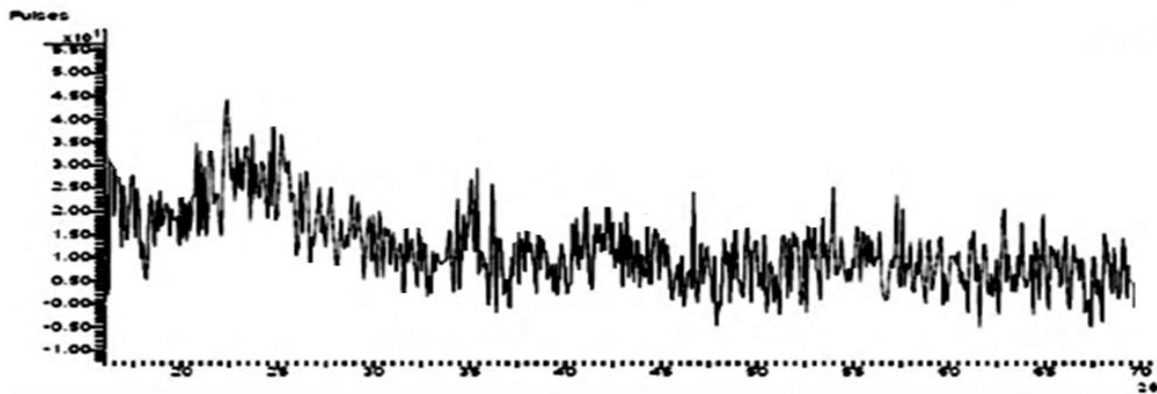


Figure 2: X-ray diffraction pattern of Cd_{0.6}Zn_{0.4}S nano-crystals.

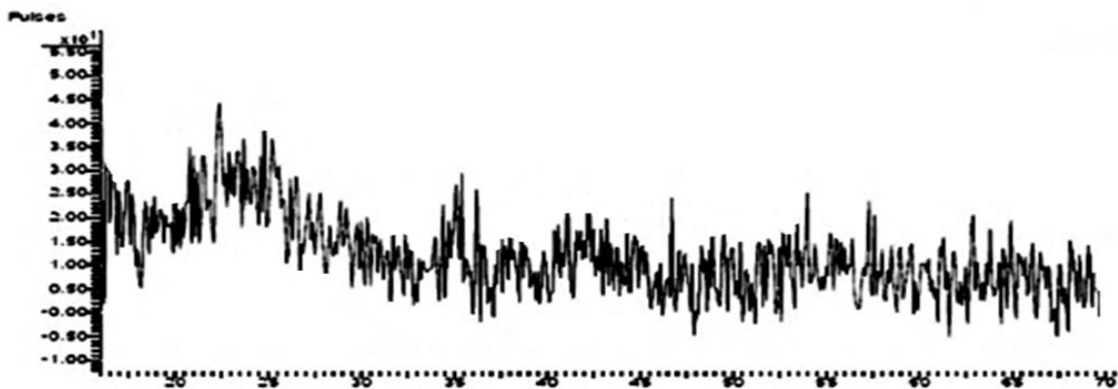


Figure 3: X-ray diffraction pattern of Cd_{0.6}Zn_{0.4}S nano-crystals.

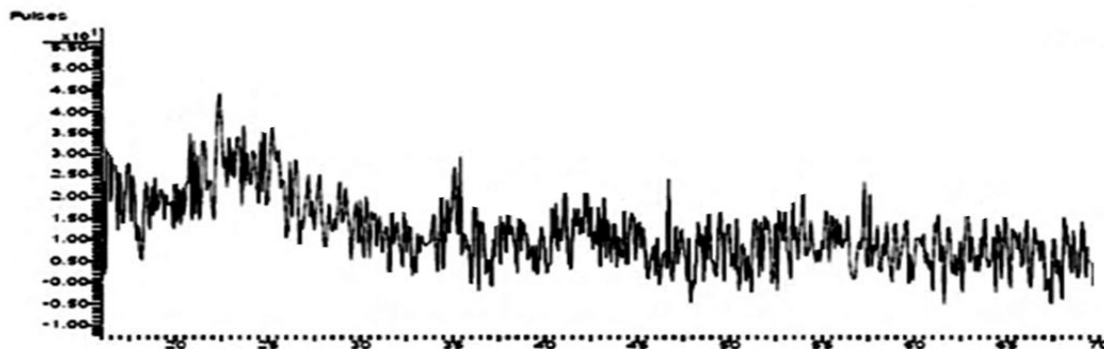


Figure 4: X-ray diffraction pattern of Cd_{0.8}Zn_{0.2}S nano-crystals

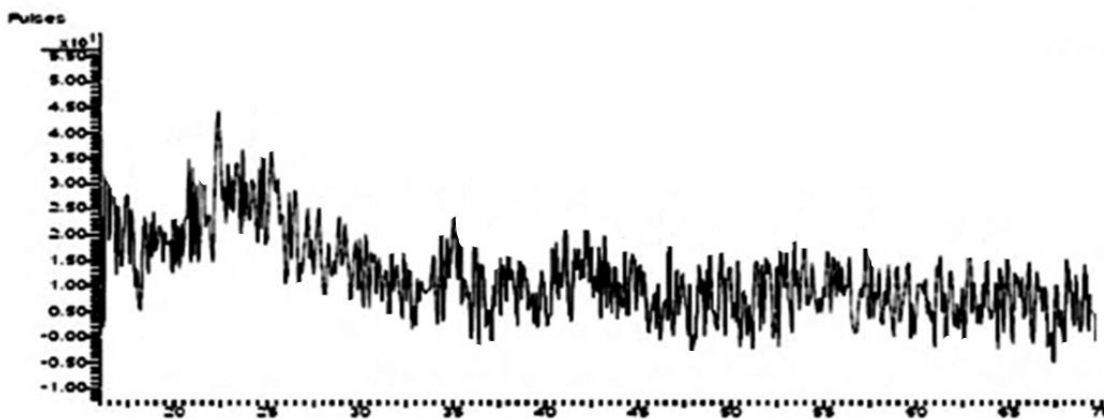


Figure 5: X-ray diffraction pattern of Cd_{1.0}Zn_{0.0}S nano-crystals

The lattice constant a and c for hexagonal planes of the Cd_{1-x}Zn_xS thin films are calculated from XRD data using the following equation.

$$\frac{1}{d^2} = \frac{4}{3} \left[\frac{l^2}{a^2} + \frac{hk^2}{c^2} \right]$$

The grain size was calculated from XRD data using Scherrie's formula (Vidya et al, 2012).

$$D = \frac{K\lambda}{\beta \cos \theta}$$

The values of a and c of Cd_{1.0}Zn_{0.0}S are 4.18 Å and 6.72 Å, respectively. The lattice constants decreased linearly with the increasing Zn concentration. This decrease in the value of 'c' is due to the Zn²⁺ incorporated in the CdS lattice entering into lattice and/or interstitial sites because of the smaller radius of Zn²⁺ ion (0.74Å) compared with that of Cd²⁺ (0.97 Å) (Nagamani et al, 2012).

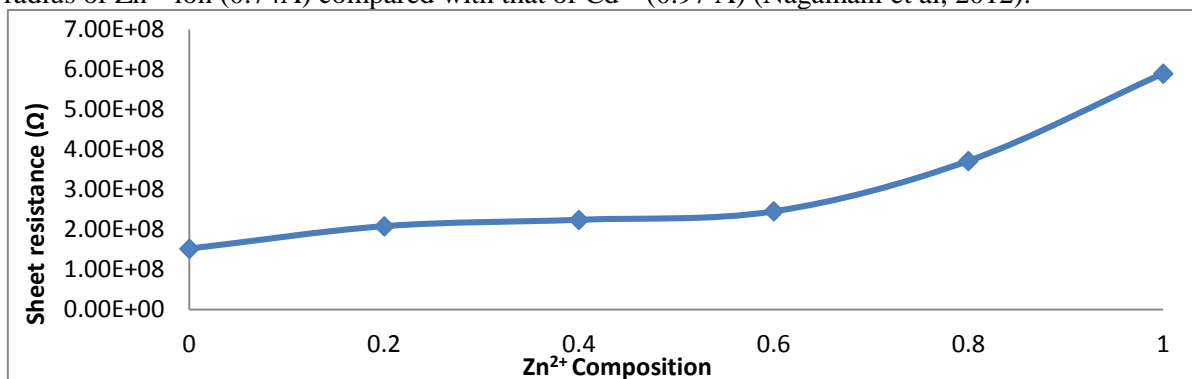


Figure 7: Plot of sheet resistance versus Zn²⁺ composition spectral of Cd_{1-x}Zn_xS nano -structured.

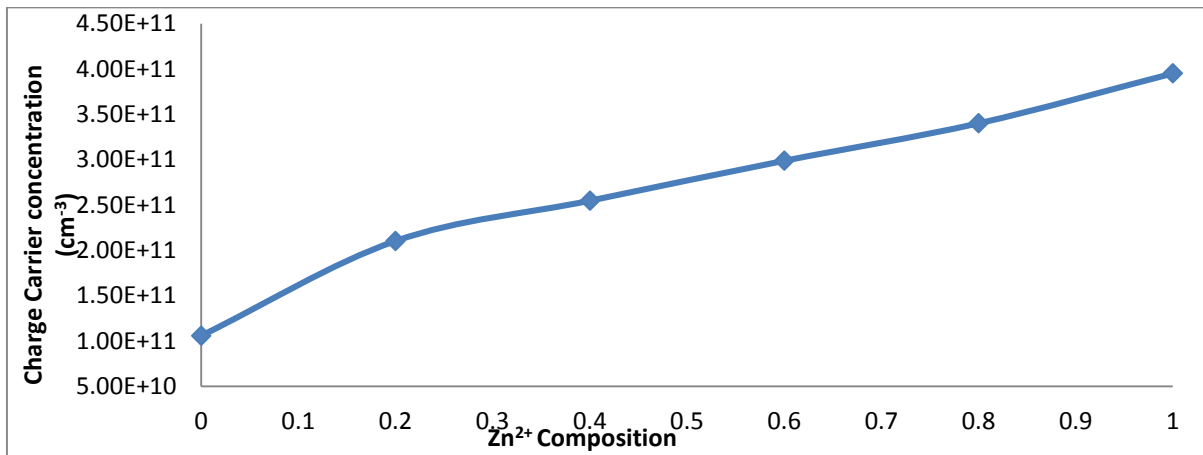


Figure 8: Plot of carrier concentration versus Zn²⁺ composition spectral of Cd_{1-x}Zn_xS nano structured.

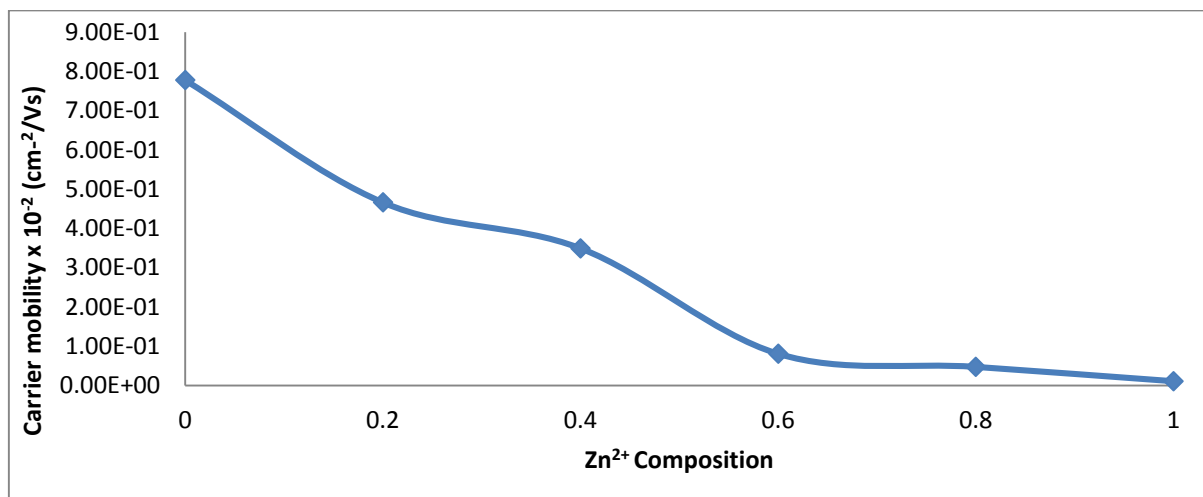


Figure 9: Plot of carrier mobility versus Zn²⁺ composition spectral of Cd_{1-x}Zn_xS nano-structured.

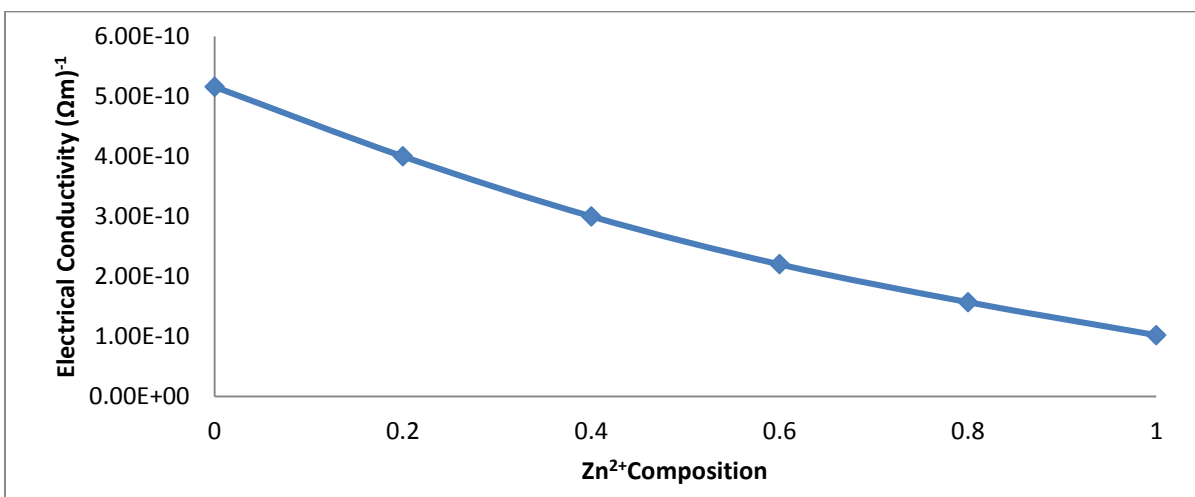


Figure 10: Plot of electrical conductivity versus Zn²⁺ composition spectral of Cd_{1-x}Zn_xS nano-structured.

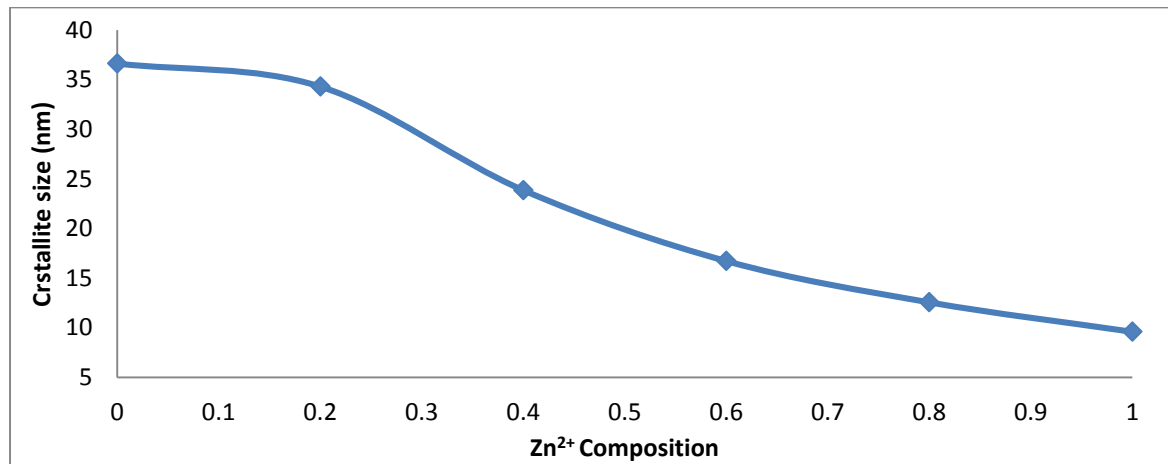


Figure 11: Plot of grain size with Zn²⁺ composition spectral of Cd_{1-x}Zn_xS nano-structured.

The electrical conductivity in these samples decrease with increasing Zn concentration in CdS as shown in figure 10. The conductivity is of order 10⁻¹⁰ which decreases with the increase of Zn concentration. This decrease in the electrical conductivity can be attributed to the effect of grain size. The grain size of these films decreases with increasing Zn content as shown in figure 11. The smaller grain sizes, which increase the grain boundary surface area are responsible for the decrease of carrier mobility. The type of carriers found in CdZnS thin films are electrons n-type which was determined from conductivity measurement.

The carrier mobility (μ) and carrier concentration (n) of Cd_{1-x}Zn_xS crystals are illustrated in figure 9 and figure 8 which were determined from Van der pauw four point probe configuration. The carrier mobility were evaluated using formula below

$$\mu = \frac{\sigma}{e.n}$$

The carrier concentrations for all Cd_{1-x}Zn_xS samples were evaluated from equation

$$n = \frac{1}{eR_H}$$

It was observed that the carrier mobility decreases and carrier density increases with increasing Zn content in CdS as shown in figure 9 and 8 respectively. These can be attributed to the increase of stacking fault density and misorientation of the crystallites (Kazmerski et al, 1992). This shows that as the Zn concentration increases the inter-grain barrier height increases (Metin et al, 2002), which is caused by the decrease of grain size. The increase of Zn concentration in CdS makes the lattice structure more and more disordered, and this is responsible for the increase of grain boundary scattering and hence the carrier mobility and electrical conductivity are diminished.

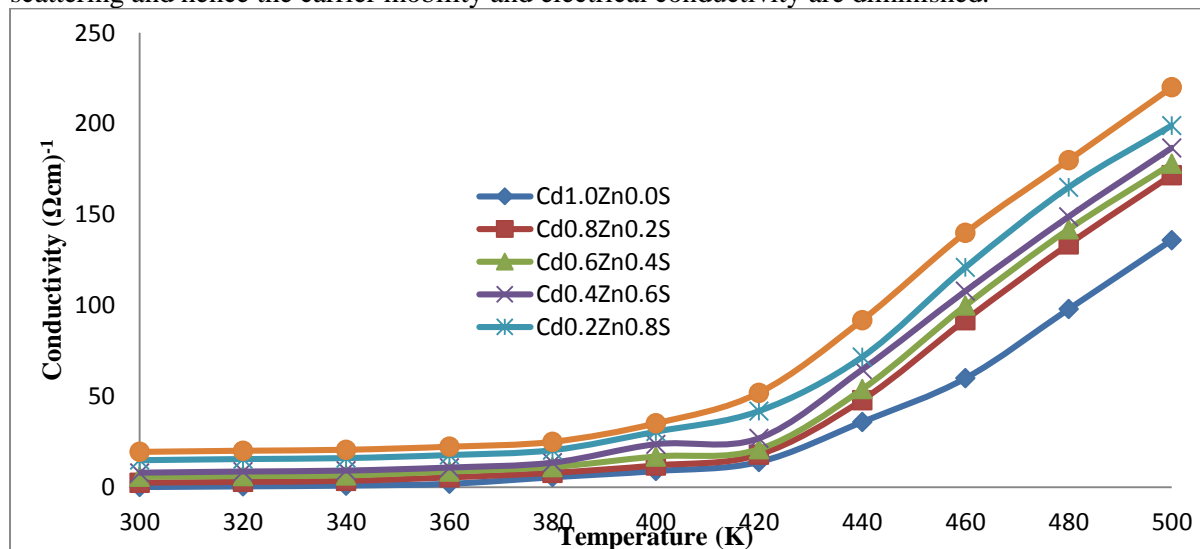


Figure 12: The temperature dependence of electrical conductivity of Cd_{1-x}Zn_xS nano-structured (0.0 ≤ x ≤ 1.0).

The conductivity increases with increasing temperature. It is observed that conductivity increases non-linearly with increase of temperature for all compositions. The increase in temperature affects the structure of nanoparticles because of the increase in the grain size, removal of defects on the surface of films and decrease of grain boundary area. This can be related to the migration of smaller crystallites and joining of similarly oriented grains. This brings a decrease in scattering of electrons, which leads to an increase of mobility of charge carriers. It is also noticed that the carrier concentration increases with increase of temperature, which is responsible for the non-linear increase of conductivity with temperature (Patidar et al, 2007).

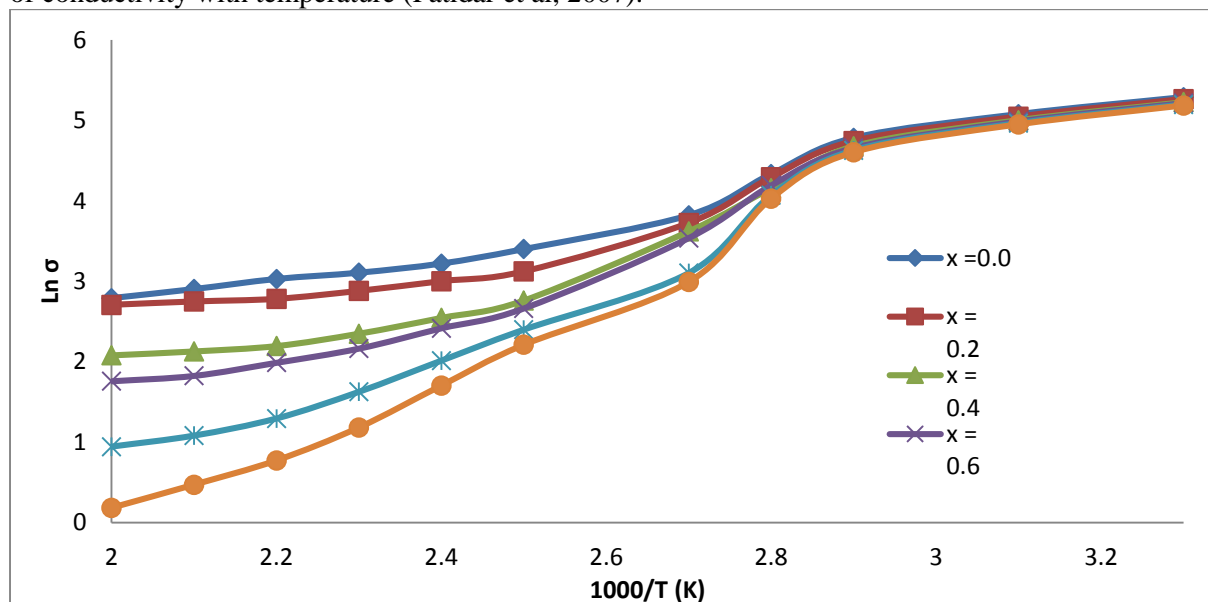


Figure 13: Variation of $\text{Ln}\sigma$ and $1000/T$ of $\text{Cd}_{1-x}\text{Zn}_x\text{S}$ nano-crystals.

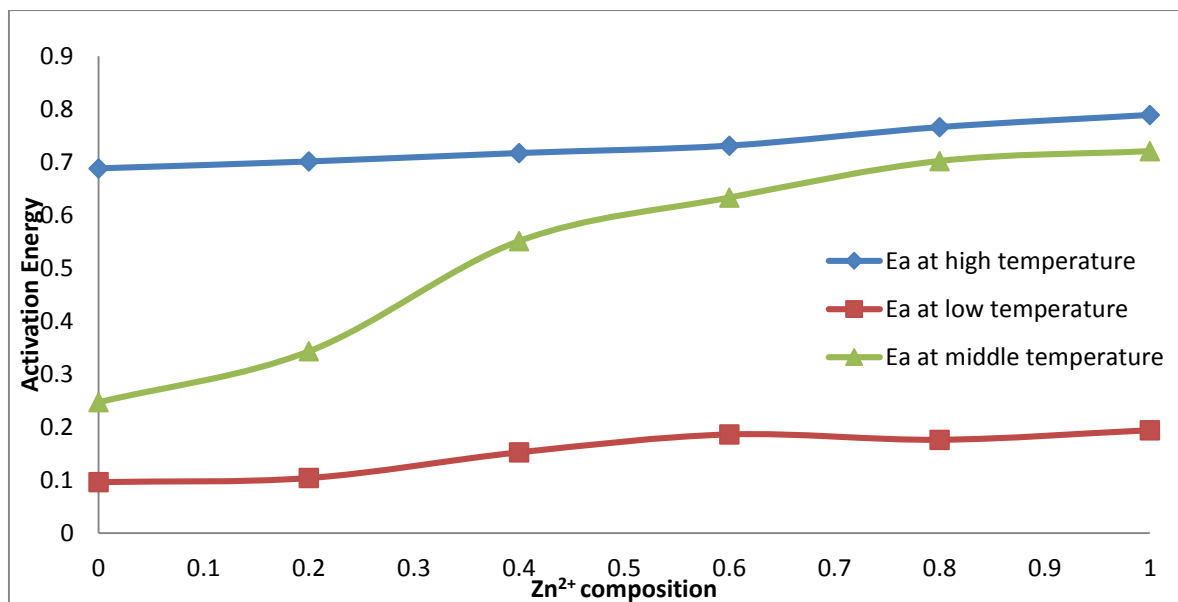


Figure 14: Variation of activation energy and Zn composition of $\text{Cd}_{1-x}\text{Zn}_x\text{S}$ nano-crystals.

Figures 13 show the plot between $\text{Ln}\sigma$ and $1000/T$ for all the samples. The activation energy has been determined using the slope determined from linear regions for each composition. It was found that the activation energy of $\text{Cd}_{1-x}\text{Zn}_x\text{S}$ nano-crystals increases forming three linear regions with increasing Zn concentration as shown in the figures. An increase in the activation energy of $\text{Cd}_{1-x}\text{Zn}_x\text{S}$ nano-crystals with the increasing concentration of Zn in CdS is used to suggest that the conduction is due to thermally assisted tunneling of the charge carriers in the localized state which are present in the band gap.

It is observed that the electrical conductivity increases with increase in temperature indicating that the film samples are semiconducting. The low values of the room temperature electrical conductivities can be attributed to the dislocations and imperfections of the films. The activation energies (E_a) were calculated by Arrhenius equation given by:

$$\sigma = \sigma_0 \exp \frac{-E_a}{K_B T}$$

The first at lower temperatures may be due to the transitions from the impurity levels in the band gap to the bottom of the conduction band or the top of the valence band. The second at middle temperature is attributed to electron or hole transitions to the conduction or valence band. The third at higher temperatures is due to the electron transitions through the extended states in the conduction band (Al-Ani et al, 1993). The activation energy in the high temperature region was found to be in the range of 0.688 to 0.787 eV. In the low temperature region, low activation energy in the range 0.0963 to 0.194eV is required for conduction. The activation energy first increased from 0.0963eV ($x = 0.0$) to 0.186eV ($x = 0.6$) and later decreased to 0.176eV ($x = 0.8$) which finally increased to 0.194eV ($x = 1.0$). In the middle temperature region, E_a increased from 0.247eV to 0.7206eV ($x = 0.8$) which later decreased to 0.8206eV ($x = 1.0$).

III. CONCLUSIONS

The XRD results showed that the grain size decreased with increasing Zn content in CdS. The structural and electrical properties of CdS are found to be zinc doped dependent. The conductivity of CdS films decreased by Zn doping and showed a maximum values at $x = 0.0$ concentration, and it is noted that the conductivity is enhanced for the large scale of the grains of the thin films. The electrical measurements reveal that the decrease of conductivity of $Cd_{1-x}Zn_xS$ with Zn concentration is due to the reduction of grain size. The non-linear increase in the electrical conductivity with the increase of temperature is mainly due to the growth of grain size, removal of defects on the surface of the films and decrease of grain boundary area. Activation energy studies support the increase in the conductivity due to improvement in crystallinity of the films which would increase the charge carrier mobility and decrease in defect levels with increase in the Zn content. The values of the resistivity of the films meet the requirements for solar cell applications.

REFERENCES

- [1] Al-Ani S.K., Mahdi, M.A. (2012). Optical characterization of chemical bath deposition $Cd_{1-x}Zn_xS$ thin Films. *Int. J. Nanoelectronics and Materials*. 5. 11-24
- [2] Abbas, T.A. Ahmad, J.M (2013) "The Effect of Copper Doping on Some Physical Properties of Chemical Sprayed CdS Thin films", *J.of Electron Devices*, 17, 1413-1416.
- [3] Hasnat. A and Podder, J (2012) "Dielectric properties of spray pyrolysis aluminum doped cadmium sulfide (Al-doped CdS) thin films", *International. J. of Physics. Science*, 7, 6158-6161.
- [4] Jae-Hyeong Lee, Jun-Sin Yi, Kea-Joon Yang, Joon-Hoon Park, Ryum-Duk Oh, (2003) "Electrical and optical properties of boron doped CdS thin films prepared by chemical bath deposition", *Thin Solid Films*, 431 - 432, 344-348.
- [5] Jafari.A., Zakaria.A, Rizwan.Z, Sabri.G.M., (2011) "Effect of Low Concentration Sn Doping on Optical Properties of CdS Films Grown by CBD Technique", *Int. J. Molecular. Science*, 12, 6320-6328.
- [6] Kumar, P. Misra, K. Kumar, D., Dhama, N., Harma, T.P., Dixit, P.N. (2004) "Structural and optical properties of vacuum evaporated $Cd_xZn_{1-x}S$ thin films", *Optical Materials*, 27, 261-264.
- [7] Metin, B., Refik, K., Mustafa, O., (2002). *Turk J. Phys.* 26, 121
- [8] Nagamani. K., Reddy.M.V., Lingappa.Y., Ramakrishna.K.T., Reddy. R. W., Miles. (2012). Physical Properties of $Zn_xCd_{1-x}S$ Nanocrystalline Layers Synthesized by Solution Growth Method. *International Journal of Optoelectronic Engineering*, 2(2): 1-4
- [9] Patidar.D., Saxena. N.S., Kananbala Sharma, Sharma. T.P. (2007). Conduction mechanism in CdZnS thin films. *Optoelectronics and Advance materials-Rapid Communications*. 1 (7), pp 329 - 332
- [10] Ulrich.B., Tomm.J.M., Dushkina.N.M., Tomm.Y., Sakai.H., (2000) "Photoelectric dichroism of oriented thin film CdS fabricated by pulsed-laser deposition", *Solid State Communications* 116, 33-35.
- [11] kazmerski, L.L., Berry, W.B., Allen, C.W., (1992) *J. Appl.Phys.* 43, 3515.
- [12] Yamaguchi T., Matsufusa J., and Yoshida A., (1992), Optical transitions in RF sputtered $CuIn_xGa_{1-x}Se_2$ thin films, *Jpn. J. Appl. Phys.*, 31 (6A), 703-705.